.Int. J. New. Chem., 2022, Vol. 9, Issue 2, pp. 102-128

International Journal of New Chemistry

Published online in http://www.ijnc.ir/.

Open Access

Print ISSN: 2645-7236

Online ISSN: 2383-188x

Original Research

The Role of Insertion of Li atom in C_{60}-Porphyrin-Metalloporphyrin, M = (V, Cr, Ni, Cu) as dyes in the DSSC by Using the Theoretical Outlook

Manizheh Ghahramanpour[1], Saeed Jamehbozorgi[2*] and Mahyar Rezvani[2]

[1]*Department of Chemistry, Faculty of Science, Arak Branch, Islamic Azad University, Arak, Iran*

[2] *Department of Chemistry, Faculty of Science, Hamedan Branch, Islamic Azad University, Hamedan, Iran*

Received: 2020-11-27 *Accepted: 2021-06-01* *Published: 2021-11-05*

ABSTRACT

In the present investigation, density functional theory with Grimme correction and time-dependent semi-empirical ZINDO/S approaches have been employed to scrutinized supra-molecular triad system as a dye sensitizer and also effect of insertion of Li atom into the C60 cavity. The impacts of the kind of transition metal in the Porphyrin ring and insertion of Li atom in the C60 fullerene on the energies of frontier molecular orbital (FMO) and UV–Vis spectra have been considered. Structural optimizations of supra-molecular triad and quantum molecular descriptor (QMD) have been carried out through the SIESTA package. We have analyzed charge transfer between two interacting species trough well-known Mulliken, Hirshfeld and Voronoi charges analysis. In addition light-harvesting efficiency (LHE), electronic transitions, chemical hardness (η), electrophilicity index (ω), electron accepting power (ω+) have been obtained with using the Orca package. We can learn that supra-molecular triad complexes Li@C_{60}–Porphyrin–Metalloporphyrine (M = V, Cr, Ni and Cu) with low energy gap, highest light-harvesting efficiency (LHE) are outstanding efficient as Dye-sensitized solar cell (DSSC) industry.

Keywords: Dye-sensitized solar cell; encapsulation; LHE; DFT; TD-semiempirical

***Corresponding Author: Tel.: 08134494025 and 09188126257**
E-mail: sjamehbozorgi@gmail.com

Introduction

The DSSC is usually composed of three section including of a sensitizer, semiconductors such as TiO_2, a conductive substrate, electrolytes and a counter electrode[1, 2]. The central part of a DSSC is the dye or the sensitizer and to yield significant efficiency, dyes must have (i) a high absorption range in UV/Vis to the near-IR region with a remarkable molar extinction coefficient to acquire most of the sunlight, (ii) a notable intramolecular charge transfer (iii) appropriate energy levels (iv) Chemical and physical solidity [2-3]. In DSSC the highest occupied molecular orbital (HOMO) moiety of the dye must be suited below the redox couple of I^-/I^{3-}electrolyte while the lowest unoccupied molecular orbital (LUMO) of the dye must be placed above the conduction band (CB) of TiO_2 semiconductor[4]. The first high-efficiency ruthenium-based sensitizer namely cis-di (thiocyanato)-bis-(2, 2′-bipyridyl)-4, 4′-dicarboxylate Ruthenium(II) (N3), announced by Grätzel[1c]. Many efforts have been devoted to designing novel and impressive sensitizers suitable for practical use. In this regards organic sensitizers without metal atoms or with cheap metal have been considered comprehensively due to their low cost, ease of synthesis, significant molar extinction coefficient as well as adequate stability[4c]. Up till now, several organic dyes demonstrating relatively high DSSCs performance have been designed and established including coumarin[5], polyene [6], hemocyanin[7], thiophene-based[8], indoline[9], perylene[10], squaraine[11], phthalocyanine[12]. It worth mentioning that sensitizers composed of a porphyrin entity have received notable consideration owing to several main features such as photochemical and electrochemical stability, high molar extinction coefficients in the visible region, low cost and environmental friendly[13]. Furthermore various porphyrins dyes are discovered with a donor–π–acceptor (D–π–A) structures[14]. Yella et al. synthesized a D-π-A based zinc porphyrin dye (YD2-o-C8) and yielded a power conversion efficiency of 12.3% [15]. In 2014, Grazel et al. offered a benzothiadiazole as the auxiliary acceptor to the D-π-A type porphyrin sensitizer SM371 leading to the D–A–π–A kind sensitizer SM315, and the SM315-based solar cell attained the PCE of 13% compared to 12% of SM371-based cell, which is amongst one of the remarkable power conversion efficacy (PCE) for DSSCs[4c, 16]. Additionally Porphyrin sensitizers including a fluorine-substituted benzothiadiazole as auxiliary acceptor and thiophene as π bridge for implementation in DSSCs were explored both of

experimentally and theoretically by Jie and co-worker[2]. In addition time-dependent DFT (TD-DFT) computations have been previously exhibited to be impressive for the estimate and evaluate of electronic transfers in free base and *meso* replaced porphyrins[17].

As one of the most exciting explorations in fullerene knowledge, encapsulation of metal atoms into fullerene cages can tune the attributes of fullerenes and therefore has been expanded into a quite new feature of chemistry, with subsequences in such diverse areas such as superconductivity and materials chemistry[18]. The theoretical investigations of electronic structures on the C_{60} cavity and its endohedral complexes were presented by Cioslowski et al. in 1991[19]. The theoretical calculations of $Li@C_{60}$ by Pavanello et al. revealed that when Li atom is inserted into the C_{60} cage, a charge of approximately 1 *e* is transferred to the surface yielding a structure with $Li@C_{60}$−electron configuration. Besides, it has been found that the fullerene cage acts as an electron buffer and incorporates excess electrons[20]. The electron acceptor ability of $Li@C_{60}$ was considerably increased as compared to pure C_{60} fullerene[21].

In present research, theoretical study were utilized to anticipate the photovoltaic characteristics of supramolecules triad systems including of C_{60}-P-MP and $Li@C_{60}$-P-MP (M= V, Cr, Ni and Cu) and to assess their potential efficiency in solar cell applications. We hope our consequences may prepare new vision into the DSSC industry.

Computational Details

Computational approaches are strategic method for molecular design and conclusions drawn from evaluations are the best guidelines for the synthesis of new materials especially novel supra-molecules triad complexes. In this regards, the structural optimizations and electronic structure of triad systems are carried out utilizing SIESTA open source package[22]. In this package, the Kohn–Sham orbitals are expanded by using the linear composition of numeric pseudo atomic orbitals for the valence electron wave functions. The Perdew–Burke–Ernzerhof (PBE) functional[23] according to the generalized gradient approximation (GGA) was utilized to consider the exchange and connection effects of electrons and the standard norm-conserving[24]. The computations are carried out by a split-valence double-zeta plus polarization function (DZP)

functions. We applied a cut of the energy of 200 Ry for grid integration. The relaxation was employed to optimize the geometry until the Hellmann–Feynman force on each atom is less than 0.02 eV/Å. Moreover, we utilized the semi-empirical Hartree–Fock-based single configuration interaction method ZINDO utilizing ORCA software[25] which can employed to figure out the electronic transmission for selected complexes and the outcomes acquire vision on the orbitals responsible for vertical transitions[25a] but it's not suitable for geometry optimization[26]. The visualization of data were achieved through Gabedit software[27] which it capability to examination UV-Vis spectra. DFT and TD-semiempirical methods are reputable computing approaches often implemented for dyad/triad complexes as a solar cell. DFT approach for geometry optimization while TD-ZINDO/S was performed for the theoretical investigation of vertical excitation energies, electronic and absorption spectra as well as LHE[28]. The Mulliken, Hirshfeld and Voroni population analysis of all complexes were performed at the DFT level of theory. Furthermore, to evaluate the change of electronic structures in interacting entities was computed by means of Mulliken [29], Hirshfeld [30] and Voronoi [31] approaches. As depicted in Table. 1, Li@C60– Porphyrin –V Porphyrin complex as a promising candidate, based on the Mulliken, Hirshfeld and Voronoi population, 0.557 e, 0.412 e and 0.443 e have been transferred from Li@C60 to Porphyrin and V-Porphyrin moieties respectively. We can see the similar trend for other triad complexes. The obtained results of respectively Mulliken, Hirshfeld and Voronoi approaches suggest that 0.466 e, 0.320 e, 0.344 e and 0.209 e, 0.056 e, 0.077 e as well as 0.275 e, 0.133 e, 0.144 e are transferred from Li@C60 to Porphyrin and Cr-Porphyrin, Cu-Porphyrin, Ni-Porphyrin as shown in Table. 1

Results and discussion

Molecular Geometry

In this section supra-molecular triad complex comprising encapsulated Li in C_{60} fullerene cavity ($Li@C_{60}$) and Porphyrin and Metalloporphyrine are carried out to capturing photon of light. Calculations approach such as DFT and TD-ZINDO/S have been utilized for scrutinizing these supra-molecular triad complexes. In this consideration after optimization of the geometric components by using the SIESTA code, the situation of the bands in absorption spectra for triad

systems was assessed by utilizing the semi-empirical ZINDO/S approach. The triad complexes including inserted Li atom in C_{60} fullerene cavity and Porphyrin and Metalloporphyrine and are

Table 1. Comparison of charge population via Mullikene, Hirshfeld, Voronoi approaches

capable of capturing the photon of light. It is determined that the center-to-center (Ct-to-Ct)

Triad	Mulliken	Hirshfeld	Voronoi
$Li@C_{60}$-P-VP			
$Li@C_{60}$=	-0.557	-0.412	-0.443
P=	0.324	0.302	0.277
VP=	0.224	0.125	0.122
$Li@C_{60}$-P-CrP			
$Li@C_{60}$=	-0.466	-0.32	-0.344
P=	0.37	0.328	0.35
CrP=	0.095	-0.018	-0.01
$Li@C_{60}$-P-NiP			
$Li@C_{60}$=	-0.275	-0.133	-0.144
P=	0.145	0.116	0.113
NiP=	0.132	0.019	0.036
$Li@C_{60}$-P-CuP			
$Li@C_{60}$=	-0.209	-0.056	-0.077
P=	0.364	0.311	0.326
CuP=	-0.155	-0. 259	-0.254

distances were somewhat larger between Metalloporphyrine and Porphyrin compared to the distances between Porphyrin and C_{60} fullerene moieties. The Ct-to-Ct distances the metal center of Metalloporphyrine (M = V, Cr, Ni and Cu) and Porphyrin for complexes C_{60} – Porphyrin – Metalloporphyrine was assessed by SIESTA code to be 19.23, 19.10, 19.06, 19.20 Å while Ct-to-Ct between porphyrin and the center of C_{60} fullerene were 19.18, 18.98, 18.98, 18.90 Å, respectively. The Ct-to-Ct distances the metal center of Metalloporphyrine and Porphyrin for complexes $Li@C_{60}$ – Porphyrin – Metalloporphyrine (M = V, Cr, Ni, and Cu) were obtained by SIESTA code to be 19.08, 19.12, 19.06, 19.08 Å while Ct-to-Ct between Porphyrin and the

center of Li@C_{60} were 19.02, 18.93, 18.88, 18.88 Å respectively. As we can see from Table. 2 the main structural parameters such as bond length, bond angle, center to the center and edge to edge distances of triad complexes. Furthermore, the edge-to-edge distance is assessed for the mentioned triad systems. As can be seen from Table 2 the edge-to-edge distance for triad Li@C_{60} fullerene between Porphyrin and Metalloporphyrine (M = V, Cr, Ni, and Cu) were 14.14, 14.10, 14.18, and 14.21 Å whereas edge-to-edge distance for Li@C_{60} fullerene and Porphyrin were15.41, 15.39, 15.32, and 15.37 Å respectively and also the edge-to-edge distance for triad complex C_{60} fullerene cavity between Porphyrin and Metalloporphyrine (M = V, Cr, Ni, and Cu) were 14.03, 13.86, 14.18, and 14.24 Å, and edge-to-edge distance for C_{60} fullerene and Porphyrin were 15.30, 15.46, 15.44, and 15.33 Å respectively. In the optimized structures, the bond length of the metal atom (M = V, Cr, Ni, and Cu) and nitrogen atoms and the bond angle of N–M–N were attained as depicted in Table 2. Besides the M-N bond lengths for Li@C_{60} – Porphyrin – Metalloporphyrine systems (M = V, Cr, Ni, and Cu) were predicted to be 2.05, 2.04, 1.98, and 2.04 Å respectively which are in good agreement with theoretical and experimental data[28, 32].

Spectral Analysis

To scrutinize a higher light to energy conversion efficiency a sensitizer with great molar extinction coefficients and absorption in whole visible/near-IR regions is essential. UV–Vis spectra are the important criteria to assess as a sensitizer for DSSC. As we know among the different semi-empirical methods the ZINDO/S is the vital approach for describing electronic spectra which parametrized for a large numeral of atoms containing transmission metals, very effective, practical and low cost methods[33]. The mentioned method exhibited better outcomes for the transition energies to the greater excited states[34].

Table 2. The geometry parameters (bond length/Å and bond angle/°), center to the center and edge-to-edge distances of system using DFT level of theory

Triad	M-N1/M-N2/M-N3/M-N4	<N1-M-N2	<N3-M-N4	Dc1-c1	Dc2-c2	De1-e1	De2-e2
C_{60}- Porphyrin -V Porphyrin	2.05 / 2.04 / 2.05 / 2.05	178.79	178.85	19.23	19.18	14.03	15.30
C_{60}- Porphyrin -Cr Porphyrin	2.04 / 2.04 / 2.03 / 2.03	179.35	179.21	19.10	18.98	13.86	15.46
C_{60}- Porphyrin -Ni Porphyrin	1.98 / 1.98 / 1.97 / 1.97	177.99	178.07	19.06	18.98	14.18	15.44
C_{60}- Porphyrin -Cu Porphyrin	2.03 / 2.04 / 2.05 / 2.04	178.78	179.25	19.20	18.90	14.24	15.33
Li@C_{60}- Porphyrin -V Porphyrin	2.04 / 2.04 / 2.05 / 2.05	179.17	179.63	19.08	19.02	14.14	15.41
Li@C_{60}- Porphyrin -Cr Porphyrin	2.04 / 2.04 / 2.03 / 2.03	178.99	179.86	19.12	18.93	14.10	15.39
Li@C_{60}- Porphyrin -Ni Porphyrin	1.98 / 1.98 / 1.97 / 1.97	177.70	177.46	19.06	18.88	14.18	15.32
Li@C_{60}- Porphyrin -Cu Porphyrin	2.05 / 2.05 / 2.03 / 2.04	179.69	179.48	19.08	18.88	14.21	15.37

The absorbance maximum wavelength (λ_{abs}) for C_{60} – Porphyrin – Metalloporphyrine (M = V, Cr, Ni and Cu) triads are around 370-700 nm while for Li@C_{60} – Porphyrin – Metalloporphyrine (M = M = V, Cr, Ni and Cu) triads is around 500 - 600 nm, and for C_{60} – Porphyrin – Cu Porphyrin and Li@C_{60} – Porphyrin – Cu Porphyrin triads is 1194.6 and 2117.2 nm respectively as shown in Table 3 and Fig. 1. In present research maximum wavelength (λabs) with Li atom encapsulated into the C60 fullerene is indicated, and it is essential to scrutinize that all signals of maximum wavelengths (λmax) match the HOMO to LUMO (H–L) transfers, which are depicted in Table 3.

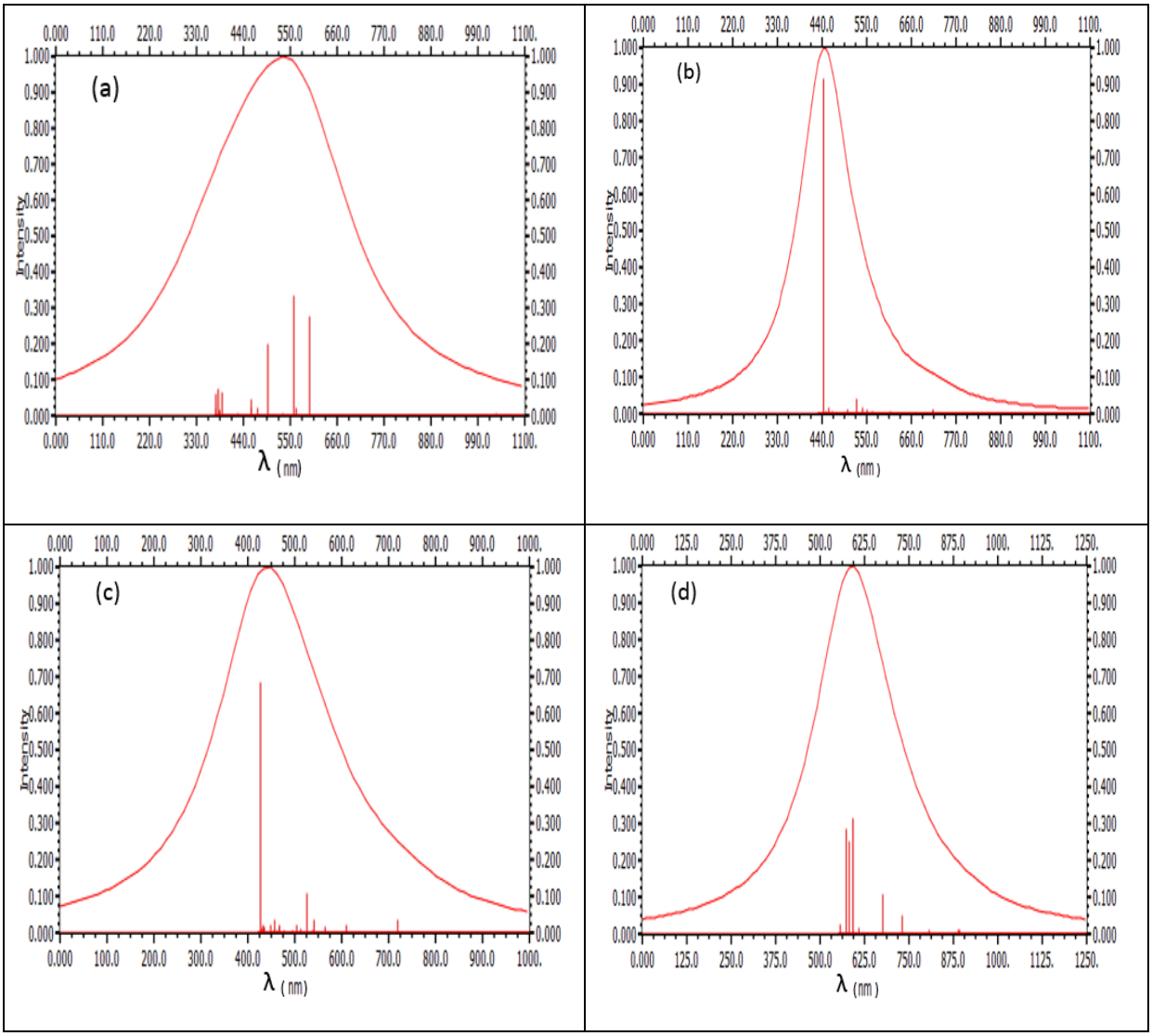
(a)
(b)
(c)
(d)
Intensity
λ (nm)

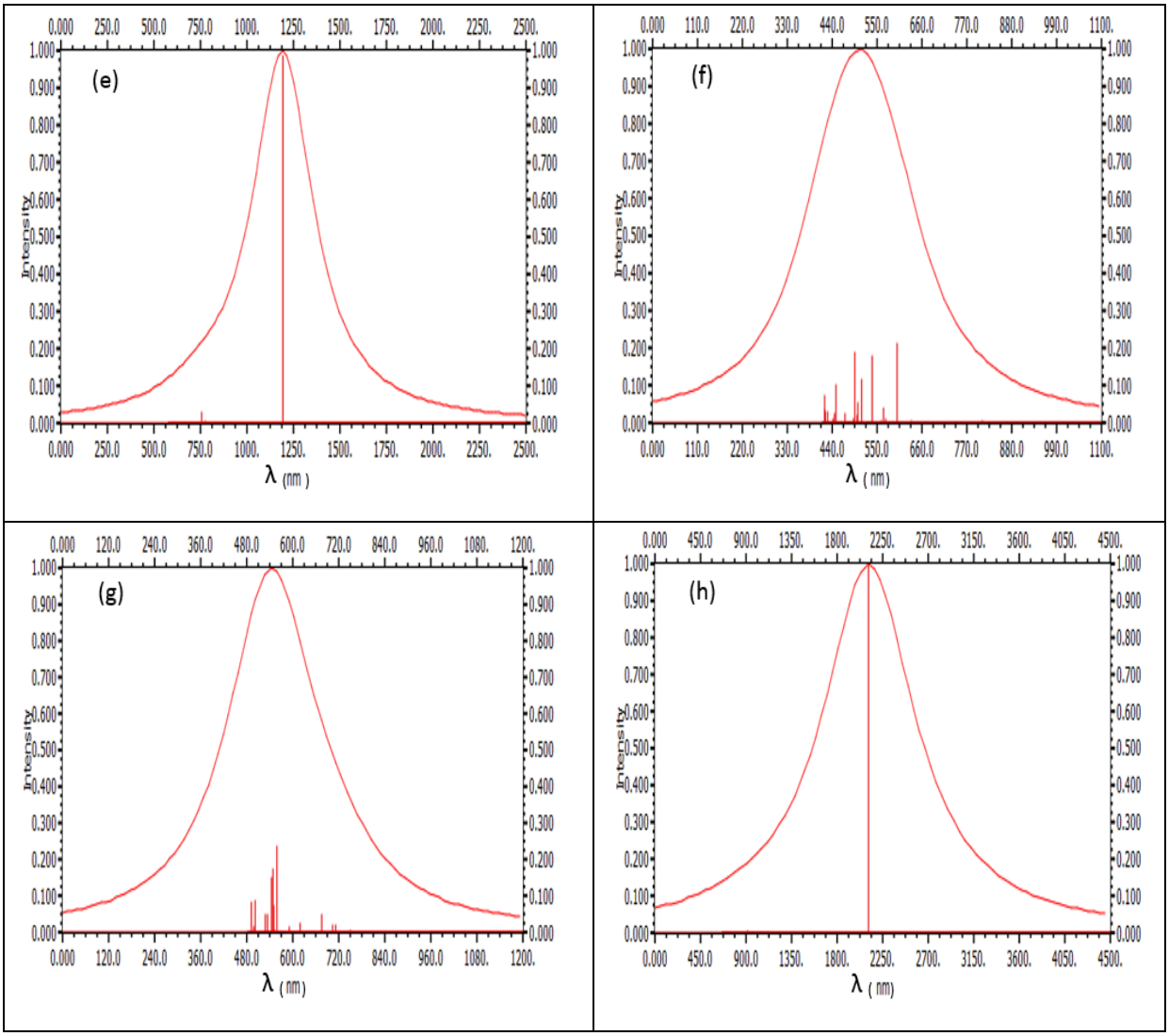

Figure 1: Simulated absorption of (a) = C_{60}-Porphyrin-V Porphyrin, (b) = C_{60}- Porphyrin -Cr Porphyrin, (c) = C_{60}- Porphyrin -Ni Porphyrin, (d) = C_{60}- Porphyrin -Cu Porphyrin, (e) = Li@C_{60}- Porphyrin -V Porphyrin, (f) = Li@C_{60}- Porphyrin -Cr Porphyrin, (g) = Li@C_{60}- Porphyrin -Ni Porphyrin, (h) = Li@C_{60}- Porphyrin -Cu Porphyrin with ZINDO/S method.

The calculated UV–Vis spectra of triad systems were computed at the ZINDO/S approach and are represented in Fig. 1. The λ_{max} of Li@ C_{60} – Porphyrin – V Porphyrin, Li@ C_{60} – Porphyrin – Cr Porphyrin, Li@ C_{60} – Porphyrin – Ni Porphyrin, Li@ C_{60} – Porphyrin – Cu Porphyrin, are observed at wavelengths 1194.6, 600.5, 559, and 2117.2 nm respectively.

In the case of Li@ C_{60} – Porphyrin – V Porphyrin complex indicated that one excited state considered at 1194.6 nm with oscillator strength of 38.16 and the molar absorbance coefficient of 1500.68. It worth mentioning that H → L (92%) form is responsible for this absorbance while in C_{60} – Porphyrin – V Porphyrin complex revealed that four excited states computed at 559.8 nm with oscillator strength of 9.66 and the molar absorbance coefficient of 178.03. In this case the H-4→ L+6 (17%), H-6→ L+4 (6%), H-6→ L+3 (5%), H-2→ L+6 (4%) configurations are responsible for this state. We utilized same trend for Li@ C_{60} – Porphyrin – Cr Porphyrin complex which exhibited that four excited states computed at 600.5 nm with oscillator strength of 5.47 and the molar absorbance coefficient of 180.18.

We can learn that H→ L +4(15%), H→ L +8(11%), H→L +4(10%), H-7 → L +5(6%) configurations are responsible for this absorption while C_{60} – Porphyrin – Cr Porphyrin complex revealed that three excited states investigated at 445.1 nm contain oscillator strength of 2.62 and the molar absorption coefficient of 38.44. In this evaluation, the H-1→ L+3 (46%), H-2→ L+2 (27%), H-4→ L+2 (6%) configurations are responsible for this state. In case of Li@ C_{60} – Porphyrin – Ni Porphyrin system discovered that five excited states calculated at 559.0 nm including oscillator strength of 4.77 and the molar absorption coefficient of 87.80. In this evaluation, the H → L + 2(14%), H -3 → L + 2 (12%), H - 7→ L + 2 (8%),H → L + 4 (5%), H → L + 19 (5%) configurations are responsible for this absorption whereas C_{60} – Porphyrin – Ni Porphyrin complex shows that four excited states computed at 427.6 nm possess oscillator strength of 0.78 and the molar absorption coefficient of 10.94. In this case, H -9→ L +1 (12%), H-9 → L +9 (9%), H -7→ L +5 (7%), H-9 → L +5 (5%) configurations are responsible for this absorption state. In addition, In case of C_{60} – Porphyrin – Cu Porphyrin system disclosed that one excited states computed at 2117.2 nm including oscillator strength of 7.12 and the molar absorption coefficient of 496.37. In this investigation, the H → L (95%) configurations are responsible for this complex. Additionally, in C_{60} – Porphyrin – Cu Porphyrin complex discovered that four excited states calculated at 594.3 nm with oscillator strength of 2.34 and the molar absorption coefficient of 45.77. In this case the H -9→ L +1 (12%), H-9 → L +9 (9%), H -7→ L +5 (7%), H-9 → L +5 (5%) configurations are responsible for mentioned state as vide in

table. 3. It worth noting that, the encapsulation of the Li atom into the C_{60} cavity can enhance the molar absorption coefficient and may be favorable for enhancing solar energy conversion efficacy. One of the crucial factor that relate to the productivity of triad systems is their efficiency in response to the light. The LHE is the part light intensity absorbed by the dye in the DSSC. Here, the LHE is explained as[35]:

$$LHE = 1 - 10^{A} = 1 - 10^{-f} \quad (1)$$

In this equation, f is the oscillator strength, which can be derived from TDZINDO/S theoretical approach. According to Eq. (1) the LHE can be directly obtained the oscillator strength and molar extinction coefficient of the sensitizer. The assessment of LHE for all triad systems are observed. As we can see from Table. 3 the greatest value of oscillator strength are related to three compounds the Li@ C_{60} – Porphyrin – Metalloporphyrine (M= V, Cr, Ni and Cu) systems.

HOMO-LUMO Density Analysis

The densities of HOMO and LUMO states of triad complexes calculated by means of TD-ZINDO/S approach are indicated in Fig. 2. Since charge-separated states are one of the main factors efficient solar cell performance. HOMOs must be localized on the donor moiety and LUMOs on the acceptor to create an effective charge isolated states[36]. The densities of HOMO and LUMO states of C_{60} – Porphyrin – Metalloporphyrine and Li@ C_{60} – Porphyrin – Metalloporphyrine triad complexes by means of TD-ZINDO/S prospect are shown in Fig. 2. From the densities of HOMO and LUMO of the Li@ C_{60} – Porphyrin – Metalloporphyrine and C_{60} – Porphyrin – Metalloporphyrine triad systems, in case of C_{60} – Porphyrin – Cr Porphyrin triad system the density of HOMO are localized in the C_{60} portion and linkage group whereas the densities of the LUMO are localized on the porphyrin moiety. We carried out same trend in Li@ C_{60} – Porphyrin – Cr Porphyrin triad system for both spin up and down states. The obtained outcomes revealed that up states the densities of HOMO are localized in the C_{60} cage unit while the densities of the LUMO are inhabited on the Cr Porphyrin portion and in case of down states HOMO are inhabited in the Cr Porphyrin segment while the densities of the LUMO are localized in the C_{60} cage unit. In the case of C_{60} – Porphyrin – Ni Porphyrin and Li@ C_{60} – Porphyrin – Ni

Porphyrin complexes, achieved results indicated that C_{60} – Porphyrin – Ni Porphyrin system the density of HOMO are centralized in the C_{60} portion and linkage group while the densities of the LUMO are inhabited on the porphyrin unit. When we encapsulated Li atom in mentioned system for up state HOMO are residing in Ni Porphyrin moiety and LUMO are localized in the C_{60} fullerene segment while for down state HOMO and LUMO are localized on C_{60} and Ni Porphyrin moieties respectively. Moreover, the same research carried out for C_{60} – Porphyrin – V Porphyrin and Li@ C_{60} – Porphyrin – V Porphyrin configurations. The achieved results show that C_{60} – Porphyrin – V Porphyrin triad systems (spin up and down states) for up state HOMO and LUMO are residing mainly in V Porphyrin while for down state HOMO are inhabited in C_{60} fullerene portion and linkage group and LUMO are residing in V Porphyrin segment whereas in case of Li@ C_{60} – Porphyrin – V Porphyrin system, HOMO and LUMO are centralized chiefly in C_{60} fullerene and V Porphyrin units. (Vide in Fig.2 a-b-g). In case of C_{60} – Porphyrin – Cu Porphyrin and Li@ C_{60} – Porphyrin – Cu Porphyrin systems, the achieved outcomes disclosed that C_{60} – Porphyrin – Cu Porphyrin system for up state, HOMO and LUMO densities are localized on the porphyrin portion and C_{60} cage unit respectively while for down state HOMO and LUMO are centralized on Porphyrin, for Li@ C_{60} – Porphyrin – Cu Porphyrin complex HOMO and LUMO are centralized in C_{60} fullerene and Cu Porphyrin unit as we can show in Fig. 2 (e-f-l).

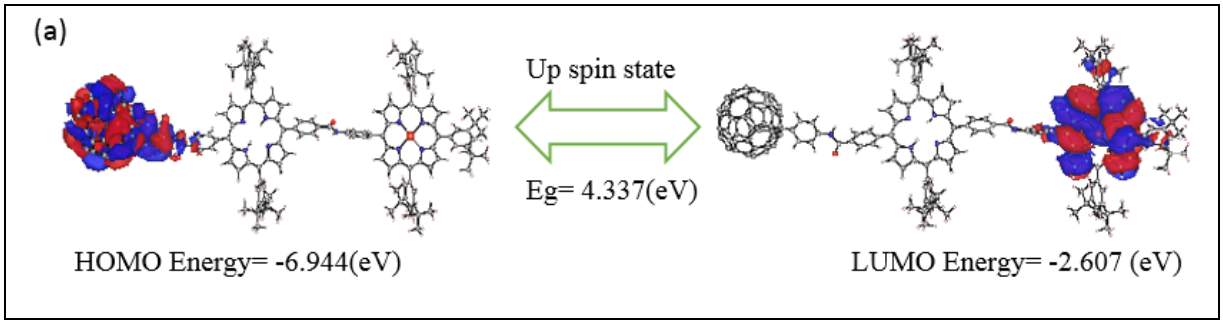

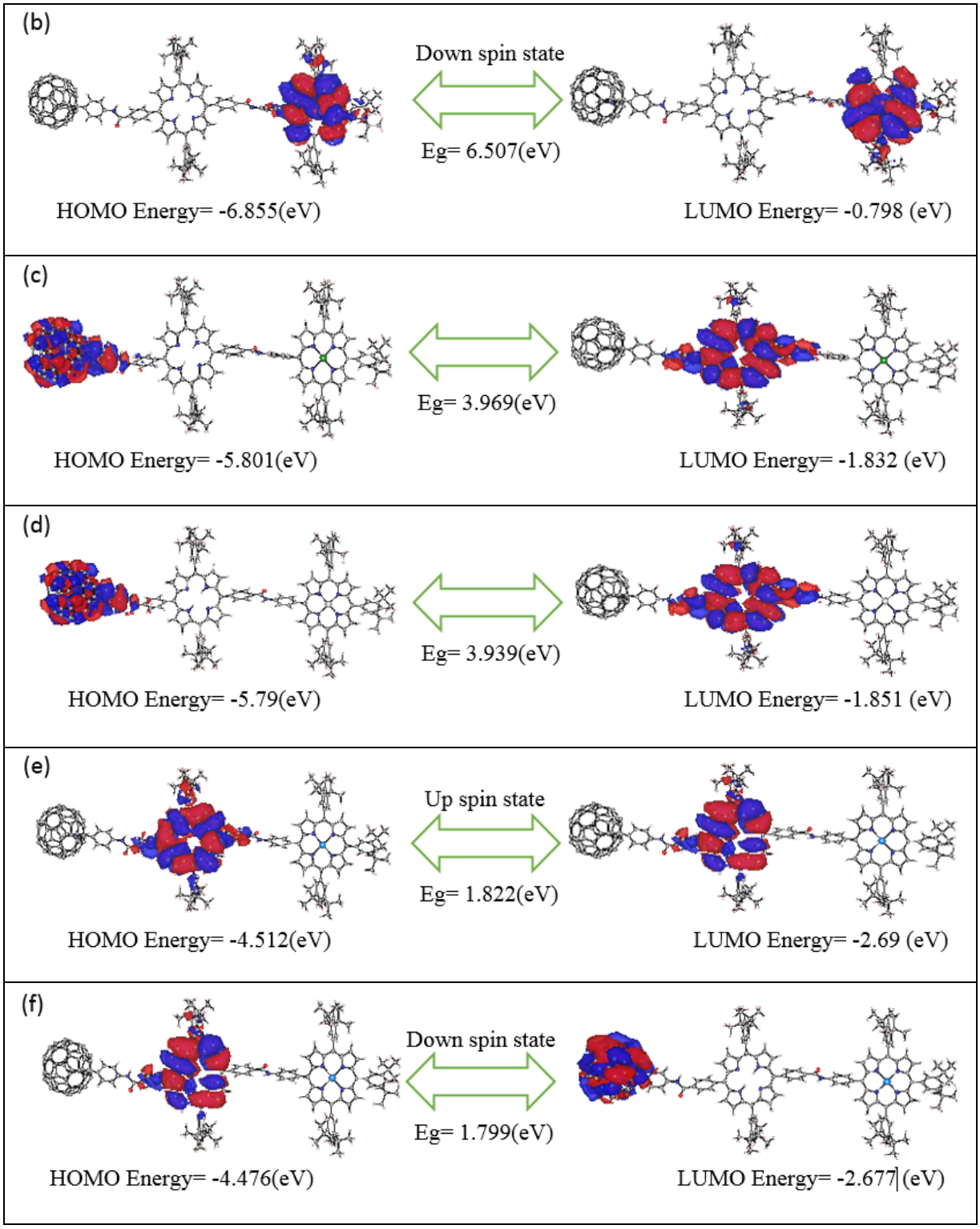
(b)
Down spin state
Eg= 6.507(eV)
HOMO Energy= -6.855(eV)
LUMO Energy= -0.798 (eV)
(c)
Eg= 3.969(eV)
HOMO Energy= -5.801(eV)
LUMO Energy= -1.832 (eV)
(d)
Eg= 3.939(eV)
HOMO Energy= -5.79(eV)
LUMO Energy= -1.851 (eV)
(e)
Up spin state
Eg= 1.822(eV)
HOMO Energy= -4.512(eV)
LUMO Energy= -2.69 (eV)
(f)
Down spin state
Eg= 1.799(eV)
HOMO Energy= -4.476(eV)
LUMO Energy= -2.677 (eV)

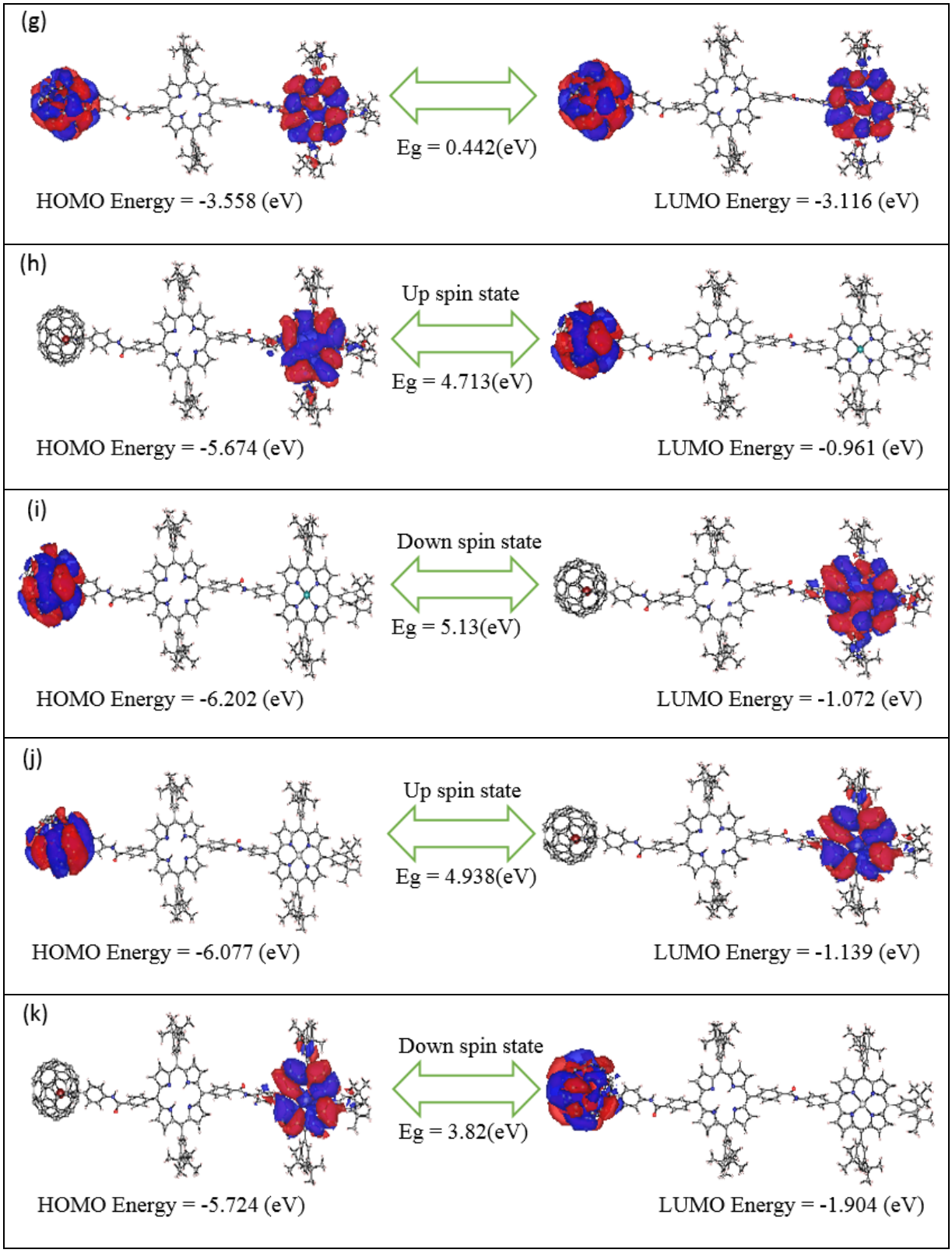
(g)
Eg = 0.442(eV)
HOMO Energy = -3.558 (eV)
LUMO Energy = -3.116 (eV)
(h)
Up spin state
Eg = 4.713(eV)
HOMO Energy = -5.674 (eV)
LUMO Energy = -0.961 (eV)
(i)
Down spin state
Eg = 5.13(eV)
HOMO Energy = -6.202 (eV)
LUMO Energy = -1.072 (eV)
(j)
Up spin state
Eg = 4.938(eV)
HOMO Energy = -6.077 (eV)
LUMO Energy = -1.139 (eV)
(k)
Down spin state
Eg = 3.82(eV)
HOMO Energy = -5.724 (eV)
LUMO Energy = -1.904 (eV)

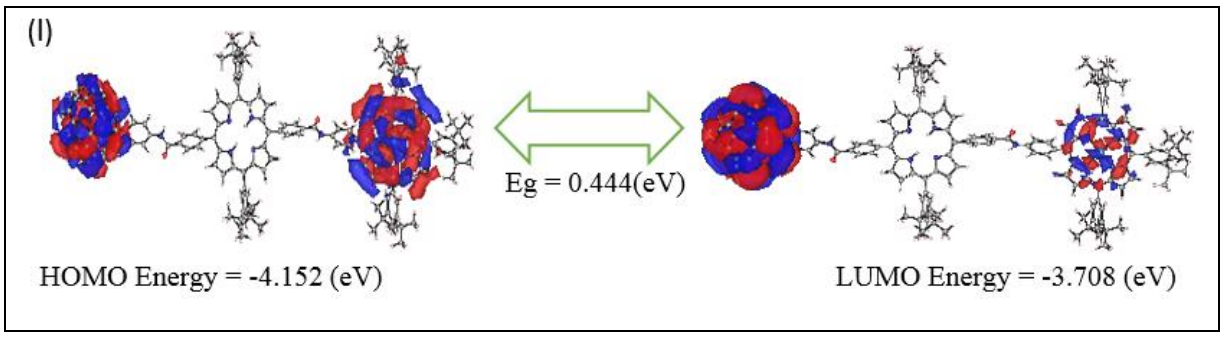

Figure 2. Calculated electron density for the (a) = C_{60}- Porphyrin -V Porphyrin $_{up}$, (b) = C_{60}- Porphyrin -V Porphyrin $_{down}$, (c) = C_{60}- Porphyrin -Cr Porphyrin, (d) = C_{60}- Porphyrin -Ni Porphyrin, (e) = C_{60}- Porphyrin -Cu Porphyrin $_{up}$, (f) = C_{60}- Porphyrin -Cu Porphyrin $_{down}$, (g) = Li@C_{60}- Porphyrin -V Porphyrin, (h) = Li@C_{60}- Porphyrin -Cr Porphyrin $_{up}$, (i) = Li@C_{60}- Porphyrin -Cr Porphyrin $_{down}$, (j) = Li@C_{60}- Porphyrin -Ni Porphyrin $_{up}$, (k) = Li@C_{60}- Porphyrin -Ni Porphyrin $_{down}$, (l) = Li@C_{60}- Porphyrin -Cu Porphyrin by using DFT-D2 method

Global Reactivity Descriptors

Quantum chemical calculations have been revealed to be very valuable for the investigation of the structural and electronic characteristics of triad complexes. Numerous efforts have been utilized to announce electronic concepts which can be exhibited in evaluating the reactivity, stability of molecular systems. Energy gap (E_g) one of the main factors in determining the electrical conductivity of the materials and can affect the photocurrent of the system. The small energy gap complex is causes the ease of transporting electrons. In the other hand, the energy of HOMO is a better assessment to the lowest ionization potential of the molecule (EI) whereas the energy of the LUMO usually is a poor evaluation to the molecule's electron affinity[37]. The complexes with higher energy gap are generally dielectric, lower energy gap are semiconductors, and directing materials have very low or no energy gap[38]. For better insight, we utilize ZINDO/S method for these considerations. The assessment of HOMO–LUMO energy-gaps (E_g) for C_{60} – Porphyrin – Metalloporphyrine systems have the following trend:

C_{60} – Porphyrin –V Porphyrin $_{(down)}$> C_{60} – Porphyrin –V Porphyrin $_{(up)}$> C_{60}– Porphyrin –Cr Porphyrin > C_{60}– Porphyrin –Ni Porphyrin > C_{60}– Porphyrin –Cu Porphyrin $_{(up)}$> C_{60}– Porphyrin –Cu Porphyrin $_{(down)}$.

While assessment HOMO–LUMO energy-gaps (Eg) for Li@C_{60}– Porphyrin –Metalloporphyrine triad systems have the following trend:

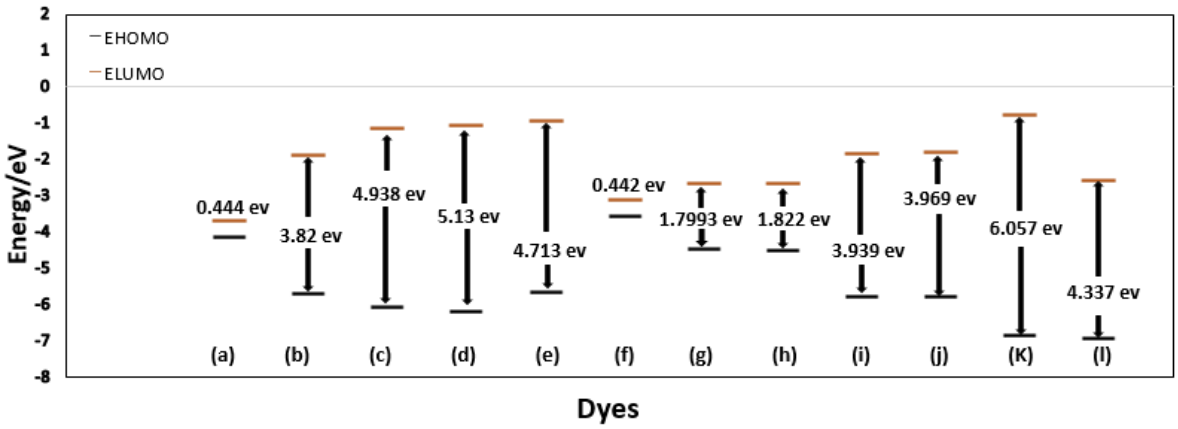

Figure 3: Schematic energy diagram of (a) = Li@C_{60}- Porphyrin -Cu Porphyrin, (b) = Li@C_{60}- Porphyrin -Ni Porphyrin $_{down}$ (c) = Li@C_{60} Porphyrin -Ni Porphyrin $_{up}$, (d) = Li@C_{60}- Porphyrin -Cr Porphyrin $_{down}$, (e) = Li@C_{60}- Porphyrin -Cr Porphyrin $_{up}$ (f) = Li@C_{60}- Porphyrin -V Porphyrin, (g) = C_{60}- Porphyrin -Cu Porphyrin $_{down}$, (h) = C_{60}- Porphyrin -Cu Porphyrin $_{up}$, (i) = C_{60}- Porphyrin -Ni Porphyrin, (j) = C_{60}- Porphyrin -Cr Porphyrin, (k) = C_{60}- Porphyrin -V Porphyrin $_{down}$, (l) = C_{60}- Porphyrin -V Porphyrin $_{up}$

Li@C_{60} –Porphyrin –Cr Porphyrin $_{(down)}$ > Li@C_{60} – Porphyrin –Ni Porphyrin $_{(up)}$ > Li@C_{60}– Porphyrin –Cr Porphyrin $_{(up)}$>Li@C_{60}– Porphyrin –Ni Porphyrin $_{(down)}$> Li@C_{60}– Porphyrin –Cu Porphyrin >Li@C_{60}– Porphyrin –V Porphyrin

We can learn that the lower energy levels HOMO and LUMO which has happened after the encapsulation lithium atom into the C_{60} fullerene in triad systems. The above mentioned compounds are suitable photosensitizer candidate due to these facts that the HOMO level is lower the redox potential of the I^-/I^{3-} electrolyte (− 4.8 eV) and the LUMO level is greater the CB of the TiO_2 semiconductor (− 4.0 eV) [100], which confirm electron injection from the dye to TiO2 and the regeneration of the triad complexes, take electrons from the electrolyte (see Fig. 3).

The gap energy computed of Li@C_{60} – Porphyrin –Metalloporphyrine systems has been meaningfully diminished and compared with other triad complexes. As we can see from Fig. 3 and Table. 4 triad complexes of Li@C_{60}– Porphyrin –Metalloporphyrine (M = V, Cr, Ni, and Cu) have the lowest energy gap. We can conclude that the encapsulation of Li atom into the C_{60}

cavity enhance conductivity of the systems such as Li@C_{60}– Porphyrin –Metalloporphyrine[39]. Consequently by means of the encapsulation of Li atom into the C_{60} cage can favorable for the solar cell applications. As we know, reduction the HOMO–LUMO energy gap of a system can harvest higher sunlight, which reasons a higher, short-circuit current density (J_{SC})[18d, 28, 32-40]. We can learn that it is a greater value of J_{SC} is favorable.

Table 3. Absorption wavelengths (in nm), energies (in eV), oscillator strength (f), molar absorption coefficient (ε), orbitals involved in the transitions and light harvesting efficacy (LHE) of triad complexes using ZINDO/S method

Triad	λ(nm)	f	E (cm^{-1})	ε	Electronic transition nature H =HOMO, L=LUMO	LHE
C_{60}-Porphyrin-V Porphyrin	559.8	9.66	17862.7	178.03	H-4→ L+6 (17%), H-6→ L+4 (6%), H-6→ L+3 (5%), H-2→ L+6 (4%)	**1**
	596.4	7.87	16767.9	154.49	H-3→ L+4 (24%), H-1→ L+3 (9%), H-6→ L+3 (5%), H-4→ L+4 (4%), H-1→ L+5 (4%)	**1**
	497.5	5.74	20101.5	93.93	H-1→ L+5 (6%), H-6→ L+6 (6%), H-5→ L+7 (5%), H-5→ L+6 (5%), H-5→ L+10 (4%)	**0.999**
	382.4	2.20	26148.5	27.70	H-4→ L+6 (6%), H-1→ L+7 (5%), H-3→ L+5 (4%)	**0.994**
	391.4	1.93	25546.3	24.87	H-6→ L+3 (5%), H-15→ L+4 (4%)	**0.988**
	376.7	1.72	26549.8	21.39	H-1→ L+4 (6%), H-9→ L+4 (4%)	**0.981**
	460.3	1.31	21726.3	19.92	H-9→ L+9 (8%), H-7→ L+4 (8%), H-6→ L+9 (5%), H-5→ L+9 (5%), H-3→ L+9 (5%)	**0.951**
C_{60}-Porphyrin-Cr Porphyrin	445.1	2.62	22466.7	38.44	H-1→ L+3 (46%), H-2→ L+2 (27%), H-4→ L+2 (6%)	**0.998**

	526.4	0.11	18997.5	1.96	H→ L+7 (13%), H→ L+11 (11%), H→ L+5 (7%), H→ L+13 (6%), H-9→ L+5 (6%)	**0.224**
C_{60}-Porphyrin-Ni Porphyrin	427.6	0.78	23385.2	10.94	H→L (64%), H-7 → L +1 (6%), -10 →L +10(4%), H-6 →L (4%)	**0.834**
	527.3	0.12	18964.8	2.12	H→L +8(12%), H→ L +11(10%), H→L +7(9%), H→L +5(7%), H→ L +13(7%), H-8 → L +5(6%)	**0.241**
C_{60}-Porphyrin-Cu Porphyrin	594.3	2.34	16825.6	45.77	H -9→ L +1 (12%), H-9 → L +9 (9%), H -7→ L +5 (7%), H-9 → L +5 (5%)	**0.995**
	573.9	2.12	17423.7	40.14	H -7 → L +6 (8%), H -15 → L (8%), H -23 → L +4 (7%), H -15 → L +2 (6%), H -2 → L (6%)	**0.992**
	584.0	1.87	17124.3	35.95	H -9→ L +2 (9%), H-7 → L +2 (7%), H -7→ L +1 (4%), H-15 → L (4%)	**0.986**
	676.8	0.80	14776.3	17.72	H -15→ L +1 (29%), H-15 → L +2 (4%), H -9→ L +9 (3%)	**0.842**
Li@ C_{60}-Porphyrin-V Porphyrin	1194.6	38.16	8371.1	1500.68	H → L (92%)	**1**
	756.4	1.28	13221.3	31.93	H→ L +25(75%), H→ L +41 (11%), H→ L +39(4%)	**0.948**
Li@ C_{60}-Porphyrin-Cr	600.5	5.47	16652.7	108.18	H→ L +4(15%), H→ L +8(11%), H→L +4(10%), H-7 → L +5(6%)	**0.999**
	496.3	4.88	20149.6	79.65	H-3 → L +4(8%), H-11 → L +4(5%), H-5 →L +7(3%)	**0.999**
	539.3	4.59	18543.2	81.56	H→ L +23(11%), H→ L +26(9%), H→L +5(7%), H→ L +8(5%)	**0.999**
	512.6	3.08	19507.0	51.99	H-5 → L +5(10%), H-5 → L +8(8%), H→L +4(7%), H-8 → L +4(4%)	**0.999**

Porphyrin						
	449.3	2.60	22257.4	38.46	H → L +13(4%), H-12 → L +7(4%), H-8 →L +8(3%), H → L +5(3%)	**0.997**
	422.6	1.87	23665.1	26.07	H-2 → L +1(30%), H-2 → L (26%), H-1 →L +1(5%), H-1 → L +16(4%), H-3 → L +3(4%)	**0.986**
	503.8	1.38	19847.5	22.97	H-7 → L +4(11%), H-12 → L +4(5%), H-3 →L +5(4%),	**0.958**
	567.3	1.08	17626.2	20.14	H→ L +8(12%), H→ L +24 (10%), H→L +9(9%), H→ L +7(6%), H→ L +11(5%)	**0.917**
Li@ C_{60}-Porphyrin-Ni Porphyrin	559.0	4.77	17888.2	87.80	H → L + 2(14%), H -3 → L + 2 (12%), H - 7→ L + 2 (8%) H → L + 4 (5%), H → L + 19 (5%)	**0.999**
	549.4	3.50	18201.4	63.40	H – 1 → L (11%), H -1 → L + 2 (10%), H - 8→ L (7%), H - 10→ L (6%), H → L + 4 (5%)	**0.999**
	545.7	2.97	18325.9	53.36	H – 4 → L + 4(19%), H -6 → L (12%), H - 6→ L + 2 (6%), H - 4→ L + 82 (4%)	**0.999**
	503.4	1.76	19864.2	29.22	H – 4 → L + 9(23%), H -3 → L + 8 (21%), H → L + 8 (7%), H → L + 33 (6%)	**0.983**
	492.3	1.71	20313.2	27.70	H – 1 → L + 2(20%), H → L + 2 (6%), H → L + 33 (6%), H - 4→ L + 5 (4 %)	**0.980**
	551.6	1.48	18127.4	26.96	H –3 → L + 4 (10%), H -1 → L +10 (9%), H - 1→ L + 6 (8%), H → L +19(8%), H -7→ L + 2 (6%)	**0.967**
Li@ C_{60}-Porphyrin-Cu Porphyrin	2117.2	7.12	4723.2	496.37	H → L (95%)	**1**

Quantum molecular descriptors (QMD) such as hardness, softness, electrophilicity, and electronegativity, which are significantly vital in modeling and insights about the reactivity of triad systems[41]. The chemical hardness (η) and softness (S) are one of the main parameters to define the stability and reactivity of the systems. It reveals resistance intramolecular charge transfer so less chemical hardness is promising whereas global softness is opposite trend to hardness[40-42]. Chemical hardness is evaluated by means of Eq. (2).

$$\eta \approx 1/2(IP - EA) \approx 1/2(E_{LUMO} + E_{HOMO}) \quad (2)$$

It can be observed that the chemical hardness of triad complexes are diminished while the conversion efficiency enhanced[42b]. Moreover, negligible amounts of η are recommended as the greatest triad complex for charge transfer thus a further short circuit current density (J_{SC}). As indicated in Table 4, the chemical hardness of Li@C_{60}– Porphyrin –Metalloporphyrine (M = V, Cr, Ni, and Cu) complexes. As seen from the Table 4, the chemical hardness of Li@C_{60}– Porphyrin –V Porphyrin (0.221 eV) and Li@C_{60}– Porphyrin –Cu Porphyrin (0.222 eV) is low which has lower resistance to intramolecular charge transfer. Consequently the order of chemical hardness is:

Li@C_{60}–Porphyrin –Cr Porphyrin $_{(down)}$>Li@C_{60}– Porphyrin –Ni Porphyrin $_{(up)}$>Li@C_{60}– Porphyrin –Cr Porphyrin $_{(up)}$>Li@C_{60}– Porphyrin –Ni Porphyrin $_{(down)}$>Li@C_{60}– Porphyrin –Cu Porphyrin >Li@C_{60}– Porphyrin –V Porphyrin

Parr and Pearson [63] defined the concept of ω as a global reactivity index which demonstrate electrophilic power of a molecule. The global electrophilicity index of a chemical species defines the electrophilic behavior of that species and greater value of ω shows higher chemical reactivity. The electron accepting power mentioned a higher ability to accept charge[43]. So the higher $\omega$and ω+are favorable. Global electrophilicity index (ω) can be assessed from the following expression as Eq. (3) and reported in Table 4.

$$\omega = \frac{\mu^2}{2\eta} \quad (3)$$

$$\omega^{+} = \frac{(I + 3A)^2}{16(I - A)} \quad (4)$$

In addition, we have considered the ω+ for triad systems as shown in Table 4. Among of them, Li@C60– Porphyrin –Cu Porphyrin and Li@C60–Porphyrin–V Porphyrin complexes had the highest ω+ value 32.848 and 23.552 eV respectively. We also observed that same trend in ω index. (Vide in Table. 4) The present study indicated that the lower chemical hardness, the higher electron accepting power, the better short-circuit current density of the Li@C60–Porphyrin –Cu Porphyrin and Li@C60– Porphyrin –V Porphyrin consequently had a better light conversion efficiency[44].

One of the most important descriptor to define the stability and reactivity of the molecules is chemical potential (μ). The tendency of an electron to escape from a complex in equilibrium in its ground state is measured by means of the chemical potential concept. If the chemical potential is greater, eventually molecule is less stable or more reactive. As can be seen from Table.4 the values calculated for Li@C60– Porphyrin –Cu Porphyrin and Li@C60– Porphyrin –V Porphyrin complexes (Stable complexes) were -3.930 and -3.337 eV respectively.

Table 4. The calculated QMD for triad complexes by ZINDO/S method

Triad	E_{HOMO}	E_{LUMO}	Gap	μ (eV)	X	η	ω	ω^{+}
C_{60}-Porphyrin-V Porphyrin	UP= -6.944	-2.607	4.337	-4.776	4.776	2.169	5.258	3.141
	Down= -6.855	-0.798	6.057	-3.827	3.827	3.029	2.417	0.883
C_{60}-Porphyrin-Cr Porphyrin	-5.801	-1.832	3.969	-3.816	3.816	1.984	3.670	2.010
C_{60}-Porphyrin-Ni Porphyrin	-5.79	-1.851	3.939	-3.820	3.820	1.969	3.705	2.041
C_{60}-Porphyrin-Cu Porphyrin	Up= -4.512	-2.69	1.822	-3.601	3.601	0.911	7.117	5.430
	Down= -4.476	-2.677	1.799	-3.576	3.576	0.900	7.110	5.434
Li@ C_{60}-Porphyrin-V Porphyrin	-3.558	-3.116	0.442	-3.337	3.337	0.221	25.194	23.552
Li@ C_{60}-Porphyrin-Cr Porphyrin	Up= -5.674	-0.961	4.713	-3.318	3.318	2.356	2.335	0.971
	Down= -6.202	-1.072	5.13	-3.637	3.637	2.565	2.578	1.080
Li@ C_{60}-Porphyrin-Ni Porphyrin	Up= -6.077	-1.139	4.938	-3.608	3.608	2.469	2.636	1.141
	Down= -5.724	-1.904	3.82	-3.814	3.814	1.91	3.808	2.140

Li@ C_{60}-Porphyrin-Cu Porphyrin	-4.152	-3.708	0.444	-3.93	3.93	0.222	34.786	32.848

Conclusion

In conclusion, the theoretical methods have been implemented to predict the photovoltaic characteristics of triad systems and to assess their potential efficiency in the solar cells applications. Detailed study of the geometrical structures and electronic features of all complexes such as molecular structures, molecular orbital energy gaps as well as HOMO and LUMO densities, UV–Vis spectra, the ground state attributes of systems have been considered by means of theoretical computations. The influences of the type of transition metal such as V, Cr, Ni and Cu in the Porphyrin ring, and encapsulation of Li atom into the C_{60} cavity on the energies of frontier molecular orbital and UV–Vis spectra have been scrutinized by using DFT ZINDO/S method. Additionally, several main parameters such as excitation energies, maximum wavelength, oscillator strength, and LHE have been assessed via the semi-empirical ZINDO/S method. The spectra for C_{60}– Porphyrin –Metalloporphyrine triad systems have been observed in the range 370 –700 nm while for Li@C_{60}– Porphyrin –Metalloporphyrine complexes in the range 500–2117.2 nm have appeared. The LHE amounts of C_{60}– Porphyrin –Metalloporphyrine triad complexes are in the range of 0.224–1% whereas the LHE amount of Li@C_{60}– Porphyrin –Metalloporphyrine systems are in the range of 0.917–1%. The obtained results showed that triad systems Li@C_{60}– Porphyrin – Metalloporphyrine (M = V, Cr, Ni, and Cu) with low energy gap make these potential triad system in photovoltaic applications and are also an excellent efficient as DSSC. Among of them, Li@C_{60}– Porphyrin –Cu Porphyrin and Li@C_{60}– Porphyrin –V Porphyrin are promising candidate to solar cell industry owing to low energy gap and hardness and high electrophilicity and electro accepting power. It worth mentioning that Li@C_{60}– Porphyrin –V Porphyrin complex due to its location in the UV-Vis region, it can be a good candidate in the solar cell application.

References

[1] M. Grätzel, Nature, 414, 338. (2011); bP.V. Kamat, J. Phys. Chem. C, 111, 2834. (2007); cC.Y. Chen, S.J. Wu, J.Y. Li, C.G. Wu, J.G. Chen and K.C. Ho, Adv. Mater., 19, 3888. (2007); R. Ghiasi, M. Manoochehri and R. Lavasani, Russian Journal of Inorganic Chemistry, 61, 1267. (2016).

[2] J. Jie, Q. Xu, G. Yang, Y. Feng and B. Zhang, Dyes Pigm., 174, 107984. (2020).

[3] K. Portillo-Cortez, A. Martinez, A. Dutt and G. Santana, J. Phys. Chem. A, 123, 10930. (2019).

[4] M. Grätzel, J. Photochem. Photobiol., A, 164, 3. (2004); bL.-L. Li, Y.-C. Chang, H.-P. Wu and E.W.-G. Diau, Int. Rev. Phys. Chem., 31, 420. (2012); cY. Guo, X. Lu, G. Li, L. Zhao, S. Wei and W. Guo, J. Photochem. Photobiol., A, 332, 232. (2017).

[5] A. Mishra, M.K. Fischer and P. Bäuerle, Angew. Chem. Int. Ed., 48, 2474. (2009); bZ.S. Wang, Y. Cui, K. Hara, Y. Dan-oh, C. Kasada and A. Shinpo, Adv. Mater., 19, 1138. (2007).

[6] H. Im, S. Kim, C. Park, S.-H. Jang, C.-J. Kim, K. Kim, N.-G. Park and C. Kim, Chem. Commun., 46, 1335. (2010).

[7] Y.-S. Chen, C. Li, Z.-H. Zeng, W.-B. Wang, X.-S. Wang and B.-W. Zhang, J. Mater. Chem., 15, 1654. (2005).

[8] G. Zhang, H. Bala, Y. Cheng, D. Shi, X. Lv, Q. Yu and P. Wang, Chemical Communications, 2198. (2009).

[9] D. Kuang, S. Uchida, R. Humphry-Baker, S.M. Zakeeruddin and M. Grätzel, Angew. Chem. Int. Ed., 120, 1949. (2008).

[10] C. Li, J.H. Yum, S.J. Moon, A. Herrmann, F. Eickemeyer, N.G. Pschirer, P. Erk, J. Schöneboom, K. Müllen and M. Grätzel, ChemSusChem, 1, 615. (2008).

[11] J.-H. Yum, P. Walter, S. Huber, D. Rentsch, T. Geiger, F. Nüesch, F. De Angelis, M.

Grätzel and M.K. Nazeeruddin, J. Am. Chem. Soc., 129, 10320. (2007).

[12] J.J. Cid, M. García-Iglesias, J.H. Yum, A. Forneli, J. Albero, E. Martínez-Ferrero, P. Vázquez, M. Grätzel, M.K. Nazeeruddin and E. Palomares, Chem. Eur. J., 15, 5130. (2009).

[13] D. Vijay, E. Varathan and V. Subramanian, J. Mater. Chem. A, 1, 4358. (2013).

[14] C.-L. Wang, J.-Y. Hu, C.-H. Wu, H.-H. Kuo, Y.-C. Chang, Z.-J. Lan, H.-P. Wu, E.W.-G. Diau and C.-Y. Lin, Energy & Environmental Science, 7, 1392. (2014); bN.V. Krishna, J.V.S. Krishna, S.P. Singh, L. Giribabu, L. Han, I. Bedja, R.K. Gupta and A. Islam, The Journal of Physical Chemistry C, 121, 6464. (2017); cJ. Luo, M. Xu, R. Li, K.-W. Huang, C. Jiang, Q. Qi, W. Zeng, J. Zhang, C. Chi and P. Wang, Journal of the American Chemical Society, 136, 265. (2014); dY. Lu, H. Song, X. Li, H. Ågren, Q. Liu, J. Zhang, X. Zhang and Y. Xie, ACS applied materials & interfaces, 11, 5046. (2019); eK. Zeng, Y. Lu, W. Tang, S. Zhao, Q. Liu, W. Zhu, H. Tian and Y. Xie, Chemical science, 10, 2186. (2019); fK. Zeng, W. Tang, C. Li, Y. Chen, S. Zhao, Q. Liu and Y. Xie, Journal of Materials Chemistry A, 7, 20854. (2019); gY. Lu, Q. Liu, J. Luo, B. Wang, T. Feng, X. Zhou, X. Liu and Y. Xie, ChemSusChem, 12, 2802. (2019).

[15] A. Yella, H.-W. Lee, H.N. Tsao, C. Yi, A.K. Chandiran, M.K. Nazeeruddin, E.W.-G. Diau, C.-Y. Yeh, S.M. Zakeeruddin and M. Grätzel, science, 334, 629. (2011).

[16] S. Mathew, A. Yella, P. Gao, R. Humphry-Baker, B.F. Curchod, N. Ashari-Astani, I. Tavernelli, U. Rothlisberger, M.K. Nazeeruddin and M. Grätzel, Nature chemistry, 6, 242. (2014).

[17] S.J. Lind, K.C. Gordon, S. Gambhir and D.L. Officer, Physical Chemistry Chemical Physics, 11, 5598. (2009).

[18] X. Lu, L. Feng, T. Akasaka and S. Nagase, Chemical Society Reviews, 41, 7723. (2012); bM.N. Chaur, F. Melin, A.L. Ortiz and L. Echegoyen, Angewandte Chemie International Edition, 48, 7514. (2009); cD. Bethune, R. Johnson, J. Salem, M. De Vries and C. Yannoni,

Nature, 366, 123. (1993); dT. Hirata, R. Hatakeyama, T. Mieno and N. Sato, Journal of Vacuum Science & Technology A: Vacuum, Surfaces, and Films, 14, 615. (1996).

[19] J. Cioslowski and E.D. Fleischmann, The Journal of chemical physics, 94, 3730. (1991).

[20] M. Pavanello, A.F. Jalbout, B. Trzaskowski and L. Adamowicz, Chemical physics letters, 442, 339. (2007); bH. Malani and D. Zhang, The Journal of Physical Chemistry A, 117, 3521. (2013).

[21] S. Aoyagi, E. Nishibori, H. Sawa, K. Sugimoto, M. Takata, Y. Miyata, R. Kitaura, H. Shinohara, H. Okada and T. Sakai, Nature chemistry, 2, 678. (2010); bS. Aoyagi, Y. Sado, E. Nishibori, H. Sawa, H. Okada, H. Tobita, Y. Kasama, R. Kitaura and H. Shinohara, Angewandte Chemie, 124, 3433. (2012); cS. Fukuzumi, K. Ohkubo, Y. Kawashima, D.S. Kim, J.S. Park, A. Jana, V.M. Lynch, D. Kim and J.L. Sessler, Journal of the American Chemical Society, 133, 15938. (2011); dK. Ohkubo, Y. Kawashima and S. Fukuzumi, Chemical Communications, 48, 4314. (2012); eY. Kawashima, K. Ohkubo and S. Fukuzumi, The Journal of Physical Chemistry A, 116, 8942. (2012).

[22] J.M. Soler, E. Artacho, J.D. Gale, A. García, J. Junquera, P. Ordejón and D. Sánchez-Portal, Journal of Physics: Condensed Matter, 14, 2745. (2002).

[23] J.P. Perdew, Physical Review B, 33, 8822. (1986).

[24] N. Troullier and J.L. Martins, Physical review B, 43, 1993. (1991).

[25] W.P. Anderson, T.R. Cundari, R.S. Drago and M.C. Zerner, Inorganic Chemistry, 29, 1. (1990); bA.D. Becke, Physical review A, 38, 3098. (1988); cJ.P. Perdew, K. Burke and M. Ernzerhof, Physical review letters, 77, 3865. (1996); dF. Neese, Wiley Interdisciplinary Reviews: Computational Molecular Science, 2, 73. (2012).

[26] J.-F. Pan, Z.-K. Chen, S.-J. Chua and W. Huang, The Journal of Physical Chemistry A, 105, 8775. (2001).

[27] A.R. Allouche, Journal of computational chemistry, 32, 174. (2011).

[28] M. Rezvani, M.D. Ganji, S. Jameh-Bozorghi and A. Niazi, Spectrochimica Acta Part A: Molecular and Biomolecular Spectroscopy, 194, 57. (2018).

[29] R.S. Mulliken, The Journal of Chemical Physics, 23, 1833. (1955); bF.M. Bickelhaupt, N.J. van Eikema Hommes, C. Fonseca Guerra and E.J. Baerends, Organometallics, 15, 2923. (1996).

[30] F.L. Hirshfeld, Theoretica chimica acta, 44, 129. (1977).

[31] C. Fonseca Guerra, J.W. Handgraaf, E.J. Baerends and F.M. Bickelhaupt, Journal of computational chemistry, 25, 189. (2004).

[32] M. Ghahramanpour, S. Jamehbozorgi and M. Rezvani, Adsorpt., 1. (2020); bJ.W. Lauher and J.A. Ibers, Journal of the American Chemical Society, 96, 4447. (1974); cN. Verdal, P.M. Kozlowski and B.S. Hudson, The Journal of Physical Chemistry A, 109, 5724. (2005).

[33] W.P. Anderson, T.R. Cundari and M.C. Zerner, International journal of quantum chemistry, 39, 31. (1991).

[34] Z. Gong and J.B. Lagowski, Journal of Molecular Structure: THEOCHEM, 729, 211. (2005).

[35] A. Irfan and A.G. Al-Sehemi, Journal of molecular modeling, 18, 4893. (2012); bC. Qin and A.E. Clark, Chemical physics letters, 438, 26. (2007); cS. Dheivamalar and K.B. Banu, Heliyon, 5, e02903. (2019).

[36] A. Shalabi, A. El Mahdy, M. Assem, H. Taha and K. Soliman, Journal of nanoparticle research, 16, 2579. (2014).

[37] O.V. de Oliveira and A. da Silva Gonçalves, Computational Chemistry, 2, 51. (2014).

[38] A.K. Srivastava, S.K. Pandey and N. Misra, Materials Chemistry and Physics, 177, 437. (2016).

[39] R.G. Parr and R.G. Pearson, Journal of the American chemical society, 105, 7512. (1983).

[40] A. Mishra and P. Bäuerle, Angewandte Chemie International Edition, 51, 2020. (2012).

[41] H. Alavi, R. Ghiasi, D. Ghazanfari and M.R. Akhgar, Rev Roum Chim, 59, 883. (2014).

[42] J. Martínez, Chemical Physics Letters, 478, 310. (2009); bZ. Kazemi, R. Ghiasi and S. Jamehbozorgi, Journal of Nanoanalysis, 6, 121. (2019).

[43] J.L. Gazquez, A. Cedillo and A. Vela, The Journal of Physical Chemistry A, 111, 1966. (2007).

[44] R. Soto-Rojo, J. Baldenebro-López and D. Glossman-Mitnik, Physical Chemistry Chemical Physics, 17, 14122. (2015).

How to Cite This Article

Marizheh Ghahramanpour, Saeed Jamehbozorg, Mahyar Rezvani, "**The role of insertion of Li atom in C60-Porphyrin-Metalloporphyrin, M = (V, Cr, Ni, Cu) as dy es in the DSSC by using the theoretical outlook"** International Journal of New Chemistry., 2022; DOI: 10.22034/ijnc.2022.1.8